

Numerical Simulation of Neural Activity Using a Stochastic Delay Integro-differential Equation

Tiago F. Sequeira¹, Pedro M. Lima¹

¹*Centro de Matemática Computacional e Estocástica, Instituto Superior Técnico, Universidade de Lisboa
Av. Rovisco Pais, 1049 001 Lisboa, Portugal plima@math.tecnico.ulisboa.pt*

Abstract. Neural field equations (NFE) are used to model the synaptic interactions between neurons in a continuous neural network, called a neural field. This kind of integrodifferential equations proved to be a useful tool for the spatiotemporal modeling of the neuronal activity from a macroscopic point of view, allowing the study of a wide variety of neurobiological phenomena, such as the processing of sensory stimuli. The aim of the present talk is to study the effects of additive noise in two-dimensional neural fields, while taking into account finite signal transmission speed. A Galerkin-type method to approximate such models is presented, which applies the Fast Fourier Transformation to optimise the computational effort required to solve this type of equations. Numerical simulations obtained by this algorithm are presented and discussed.

Keywords: Neural field, stochastic differential equation, space-dependent delay, Galerkin method, Euler-Maruyama method.

1 Introduction

Neural field models represent the large-scale dynamics of spatially structured networks of neurons in terms of nonlinear integro-differential equations. One of the main applications of these models is related with the interpretation of experimental data, including those obtained from EEG, fMRI and optical imaging [1]. These equations also play an important role in Cognitive Robotics, since the architecture of autonomous robots, able to interact with other agents in solving a mutual task, is strongly inspired by the processing principles and the neuronal circuitry in the primate brain (see [2]).

These models first appeared in the works of Wilson and Cowan [3] and then were developed by Amari [4]. The neural field equation can be written as

$$\alpha \frac{\partial V}{\partial t}(\mathbf{x}, t) = I(\mathbf{x}, t) - V(\mathbf{x}, t) + \int_{\Omega} K(\|\mathbf{x} - \mathbf{y}\|_2) S[V(\mathbf{y}, t)] d^2\mathbf{y}, \quad (1)$$

where $V(\mathbf{x}, t)$ is the unknown function and denotes the electric potential at point \mathbf{x} and moment t ; I is an external stimulus; S is the firing rate function (represents the firing capacity of the neuron as a function of its potential). K is the connectivity function (strength of the connection between points \mathbf{x} and \mathbf{y}). In the present form of the equation, the connectivity strength is assumed to depend only on the distance between \mathbf{x} and \mathbf{y} . The constant α is related with the decay rate.

Since in (1) we assume that electric signals in the brain propagate with infinite speed, it is not always a realistic biological model. Depending on the neuron type, the axonal conduction speed can widely vary between 1 ms^{-1} to 100 ms^{-1} , originating significant time delays in different brain structures [5].

In order to take into account the delay resulting from finite propagation speed, in the integral term of equation (1) we replace $V(\mathbf{y}, t)$ by $V(\mathbf{y}, t - d)$, where $d(\mathbf{x}, \mathbf{y})$ represents the time spent time spent by a stimulus to travel from point \mathbf{y} to \mathbf{x} . This delay is assumed to be proportional to the distance $\|\mathbf{y} - \mathbf{x}\|$ and inversely proportional to the transmission speed v . Hence if v is sufficiently high, d can be neglected, and we return to the original model.

Delay can induce qualitative changes in the behaviour of solutions of the NFE. As remarked by the authors of [6], 'in case of oscillatory bifurcations, the variance of the distributed propagation and feedback delays affects the frequency of periodic solutions'.

Even in the case of infinite transmission speed, integro-differential equations in several spacial dimensions are quite a challenge for numerical simulation, because the standard approaches, based on collocation methods and quadrature rules, require a very high computational effort.

In the case of delay the difficulty increases significantly because the existence of the delay creates difficulties to the use of the discrete Fourier transform (as it will be discussed below).

Several approaches have been applied to obtain numerical solutions of the NFE, both in the case of finite and infinite transmission speed (see for example [7] and [8]). As it happens in other problems arising from Biology, taking noise into account is essential to obtain realistic models of neural activity. With this purpose, various stochastic versions of equation (1) have been introduced and many authors have analysed noise-induced changes in the behaviour of solutions of the NFE.

In [9], the authors analyse the spatiotemporal dynamics of a general integrodifferential equation, subject to additive random fluctuations, and they conclude that the global fluctuations shift the Turing bifurcation threshold.

The joint effect of noise and delay was considered in [10], where the authors consider a spatially extended neural field model involving distributed delays and observe a stochastic bifurcation induced by the additive noise.

In this paper, we follow a stochastic approach introduced by Kuehn and Riedler in [11], where the following stochastic neural Field Equation (SNFE) with additive noise is introduced:

$$\alpha dV(\mathbf{x}, t) = \left(I(\mathbf{x}, t) - V(\mathbf{x}, t) + \int_{\Omega} K(\|\mathbf{x} - \mathbf{y}\|_2) S[V(\mathbf{y}, t)] d^2\mathbf{y} \right) dt + \epsilon dW(\mathbf{x}, t). \quad (2)$$

We consider an extension of equation (2) with a delay in the kernel, which may be written as

$$\alpha dV(\mathbf{x}, t) = [I(\mathbf{x}, t) - V(\mathbf{x}, t) + A(\mathbf{x}, t)]dt + \epsilon dW(\mathbf{x}, t), \quad (3)$$

where A denotes the integral operator:

$$A(\mathbf{x}, t) = \int_{\Omega} K(\|\mathbf{x} - \mathbf{y}\|_2) S[V(\mathbf{y}, t - d(\mathbf{x}, \mathbf{y}))] d^2\mathbf{y}. \quad (4)$$

If $d \neq 0$, A is not a convolution and it is not possible to apply directly the Fourier transform to (4). With the purpose of overcoming this difficulty we use a technique first proposed by the authors of [7] in the deterministic case, which has been adapted in [12] to the stochastic equation (3). Details about this technique can be found in the cited papers.

A Julia code which implements this numerical algorithm, created by the first author of the present paper, has been described in [13]. This algorithm has been applied in [12] and [14] to simulate neural processes which involve delay and noise.

In the present work we use it to investigate the interaction between external input and noise in such processes. In Sec. 2 we briefly describe the numerical algorithm. In Sec. 3 we present and discuss numerical results, and we finish with conclusions in Sec. 4.

2 Numerical Algorithm

2.1 Expanding the Solution as a Series

Using the theoretical framework of [11], we aim to extend to the stochastic scenario the spectral numerical method developed in [7] for the deterministic case.

According to the Karhunen-Loeve formula, a stochastic process can be represented as an infinite linear combination of orthonormal functions. Thereby, we can write the solution, V , in the form:

$$V(\mathbf{x}, t) = \sum_{m=-\infty}^{\infty} \sum_{n=-\infty}^{\infty} \hat{v}_{mn}(t) \phi_{mn}(\mathbf{x}), \quad (5)$$

where $\phi_{mn}(\mathbf{x})$ denotes the basis functions, which form an orthonormal set (the choice of basis functions will be detailed in the next subsection).

Taking the inner product, in the usual sense, of both sides of (3) by the basis functions $\phi_{mn}(\mathbf{x})$, we obtain

$$\begin{aligned} \alpha \langle dV(\mathbf{x}, t), \phi_{mn}(\mathbf{x}) \rangle &= [\langle I(\mathbf{x}, t), \phi_{mn}(\mathbf{x}) \rangle - \langle V(\mathbf{x}, t), \phi_{mn}(\mathbf{x}) \rangle \\ &+ \langle A(\mathbf{x}, t), \phi_{mn}(\mathbf{x}) \rangle] dt + \epsilon \langle dW(\mathbf{x}, t), \phi_{mn}(\mathbf{x}) \rangle, \end{aligned}$$

while the stochastic term $dW(\mathbf{x}, t)$ can be written as:

$$dW(\mathbf{x}, t) = \sum_{m=-\infty}^{\infty} \sum_{n=-\infty}^{\infty} \phi_{mn}(\mathbf{x}) \lambda_{mn} d\beta_{mn}(t), \quad (6)$$

with the correlation function given by:

$$\mathbf{E}\{W(\mathbf{x}, t)W(\mathbf{y}, t)\} = \min(t, s) \frac{1}{2\xi} \exp\left(-\frac{\pi\|\mathbf{x} - \mathbf{y}\|_2^2}{4\xi^2}\right), \quad (7)$$

where the parameter ξ models the spatial length correlation. According to [11], assuming that the condition $\xi \ll L$ holds true, the form of the eigenvalues λ_{mn} of the covariance operator Q in (3), can be explicitly derived

$$\lambda_{mn} = \exp\left(-\frac{\xi^2(m^2 + n^2)}{8\pi}\right). \quad (8)$$

Substituting (8) into (6) and taking into account the orthonormality condition of the basis functions, the evolution of $\hat{v}_{mn}(t)$ are described as:

$$\alpha d\hat{v}_{mn}(t) = [\langle I(\mathbf{x}, t), \phi_{mn}(\mathbf{x}) \rangle - \hat{v}_{mn}(t) + \langle A(\mathbf{x}, t), \phi_{mn}(\mathbf{x}) \rangle] dt + \epsilon \lambda_{mn} d\beta_{mn}(t). \quad (9)$$

2.2 Basis functions

Let us adopt the same choice of the basis functions as in the works [7, 11], where they use the trigonometric functions, which can be expressed in this form:

$$\phi_{mn}(\mathbf{x}) = e^{i\mathbf{x} \cdot \mathbf{k}_{mn}}, \quad (10)$$

with i being the imaginary unit and $\mathbf{k}_{mn} = \frac{2\pi}{L}(m, n)$, $m, n \in \mathbb{Z}$ is the discrete wave vector which is implied by the periodic boundary conditions. So, with these trigonometric basis functions we can obtain $\hat{v}_{mn}(t)$ by applying Fourier Transforms to each inner product present in (9).

The functions of our problem (3) are all real, more precisely, $V, I, K, S : \mathbb{R}^k \rightarrow \mathbb{R}$, $k = 1, 2$, so their Fourier spectrum exhibits a Hermite symmetry, i.e. if f is a real function, $f : \mathbb{R} \rightarrow \mathbb{R}$ and \mathcal{F} its Fourier Transform, then $\mathcal{F}(-k) = \mathcal{F}^*(k)$, meaning that $\text{Re}(\mathcal{F}(k))$ is even and $\text{Im}(\mathcal{F}(k))$ is odd.

Having in mind (10) the series (5) is expanded as

$$\begin{aligned} V(\mathbf{x}, t) &= \sum_{m=-\infty}^{\infty} \sum_{n=-\infty}^{\infty} \hat{v}_{mn}(t) e^{i\mathbf{x} \cdot \mathbf{k}_{mn}} \\ &= \sum_{m=-\infty}^{\infty} \sum_{n=-\infty}^{\infty} \hat{v}_{mn}(t) \left[\cos\left((mx + ny)\frac{2\pi}{L}\right) + i \sin\left((mx + ny)\frac{2\pi}{L}\right) \right], \end{aligned} \quad (11)$$

now, making use of the Hermite symmetry property, $\hat{v}_{mn} = \hat{v}_{mn}^*$, we can rewrite (5) as follows:

$$V(\mathbf{x}, t) = \sum_{m=0}^{\infty} \sum_{n=0}^{\infty} c_{mn}(t) \cos\left((mx + ny)\frac{2\pi}{L}\right) + d_{mn}(t) \sin\left((mx + ny)\frac{2\pi}{L}\right), \quad (12)$$

with $c_{mn}(t) = 2\text{Re}[\hat{v}_{mn}(t)]$ and $d_{mn}(t) = 2\text{Im}[\hat{v}_{mn}(t)]$.

2.3 Fourier coefficients of A

Now, we direct our attention to the inner product $\langle A(\mathbf{x}, t), \phi_{mn}(\mathbf{x}) \rangle$. As already said, the integral operator A can be written as two convolutions, one in space and other in time. Let us rewrite A as

$$A(\mathbf{x}, t) = \frac{1}{L^2} \int_0^{\tau_{max}} \left(K_{\text{delay}}(\tau) * SV(t - \tau) \right) (\mathbf{x}) d\tau, \quad (13)$$

with the symbol $*$ denoting a convolution, which is defined by $(f * g)(x) = \int_{-\infty}^{\infty} f(x)g(x - y) dy$. At this point, we can recall the identity $\mathcal{R}\mathcal{F}(f * g) = \mathcal{R}\mathcal{F}(f) \cdot \mathcal{R}\mathcal{F}(g)$, where $\mathcal{R}\mathcal{F}$ is the Real Fourier Transform operator. So, applying this identity to (13), we can write the Fourier coefficients of the integral operator A as:

$$\hat{a}_{mn}(t) = \frac{1}{L^2} \int_0^{\tau_{max}} \mathcal{R}\mathcal{F}\left(K_{\text{delay}}(\mathbf{y}, \tau)\right) \cdot \mathcal{R}\mathcal{F}\left(SV(\mathbf{y}, t - \tau)\right) d\tau. \quad (14)$$

Finally, inserting (14) into (9) and denoting $\hat{a}_{mn} = \langle I(\mathbf{x}, t), \phi_{mn}(\mathbf{x}) \rangle$, (9) can be rewritten as

$$\alpha d\hat{v}_{mn}(t) = [\hat{a}_{mn}(t) - \hat{v}_{mn}(t) + \hat{a}_{mn}(t)] dt + \epsilon \lambda_{mn} d\beta_{mn}(t), \quad (15)$$

with $\hat{v}_{mn}(t)$, $\hat{a}_{mn}(t)$ and $\hat{a}_{mn}(t)$ being the Fourier coefficients of $V(\mathbf{x}, t)$, $I(\mathbf{x}, t)$ and $A(\mathbf{x}, t)$, respectively.

2.4 Space and time discretization

After reducing the problem to the system of equations (15), we use a discretization method, which truncates the series (5) with sufficiently large integers M and N , in order to approximate our solution $V(\mathbf{x}, t)$ with a finite sum,

$$V_{MN}(\mathbf{x}, t) = \sum_{m=0}^M \sum_{n=0}^N \hat{v}_{mn}(t) \phi_{mn}(\mathbf{x}). \quad (16)$$

The next step is to discretize the space and time domains. For that purpose let us consider the physical domain $\Omega = [-\frac{L}{2}; \frac{L}{2}]^k$, $d = 1, 2$. We can discretize Ω with a constant step $\Delta \mathbf{x} = \frac{L}{M}$, where M and N being the number of nodes in each direction, respectively. For the sake of simplicity $M = N$. Then, the discrete domain, Ω_{Δ} , is written as

$$\begin{aligned} \mathbf{x} &= \left[x_0 = -\frac{L}{2}, x_1 = -\frac{L}{2} + \Delta x, \dots, x_M = \frac{L}{2} - (M-1)\Delta x \right] \\ \mathbf{y} &= \left[y_0 = -\frac{L}{2}, y_1 = -\frac{L}{2} + \Delta y, \dots, y_M = \frac{L}{2} - (M-1)\Delta y \right], \end{aligned} \quad (17)$$

with $m = 0, \dots, M-1$. Now, considering the continuous interval $[0, T]$ and introducing the constant step $\Delta t = \frac{T}{n_t}$, we can define the mesh by setting $t_i \in [t_0 = 0, t_1 = \Delta t, \dots, T = n_t \Delta t]$.

Once the discretization is introduced, system (15) can be integrated in time using the Euler-Maruyama method (for details see [12]).

3 Numerical Simulations

In [12] and [14] a number of numerical experiments have been carried out, both to test the performance of the numerical algorithm described above and to investigate certain physical phenomena with practical interest. In particular, a neural field was investigated where the behaviour of the solution may switch from the convergence to a stable stationary state to a periodic solution. In other words, bifurcation points are observed, which are related with various parameters of the system, namely, the transmission speed, the amplitude of the external input and the level noise.

In this section, we recall the results of these simulations and add some new experiments, which lead us to interesting conclusions on the solution behaviour.

We begin by describing the problem. Let us consider equation (3) with the connectivity kernel defined by

$$K(\mathbf{x}) = \frac{20}{10\pi} \exp(-\|\mathbf{x}\|_2) - \frac{14}{18\pi} \exp\left(-\frac{\|\mathbf{x}\|_2^2}{3}\right), \quad (18)$$

the firing rate function given by the Heaviside step function,

$$S(V) = H(V - V_{th}), \quad (19)$$

and the constant external input of the form

$$I(\mathbf{x}) = I_0 \exp\left(-\frac{\|\mathbf{x}\|_2^2}{32}\right), \quad (20)$$

coupled with the initial condition $V(\mathbf{x}, t_0) = 0$, $t_0 \in [-\tau_{max}, 0]$. In all scenarios presented below the problem was solved on the spatial domain Ω of length $L = 20 \Rightarrow \Omega = [-10, 10] \times [-10, 10]$; we used a mesh with $N = 2^8 = 256$ nodes in each direction, meaning $\Delta \mathbf{x} = 0.078125$ and the time step size $\Delta t = 0.05$. The considered threshold is $V_{th} = 0.005$. We begin by analysing the case $\epsilon = 0$ (no noise).

3.1 Deterministic scenario

It has been demonstrated in [15] that the solutions to these fields are bounded, i.e. they either oscillate or tend to a stationary state. In this case we pay attention to the maximum and minimum of the solution over time, $\max_V(t) = \max_{\mathbf{x} \in \Omega} V(\mathbf{x}, t)$ and $\min_V(t) = \min_{\mathbf{x} \in \Omega} V(\mathbf{x}, t)$, respectively. Analysing how $\max_V(t)$ and $\min_V(t)$ evolve over time, allows us to find whether or not the solution has oscillatory neuronal activity.

When considering the case of finite transmission speed, the time spent to reach the stationary state (T_0) increases as v decreases. When v attains a certain critical value, the solution oscillates during all the time interval.

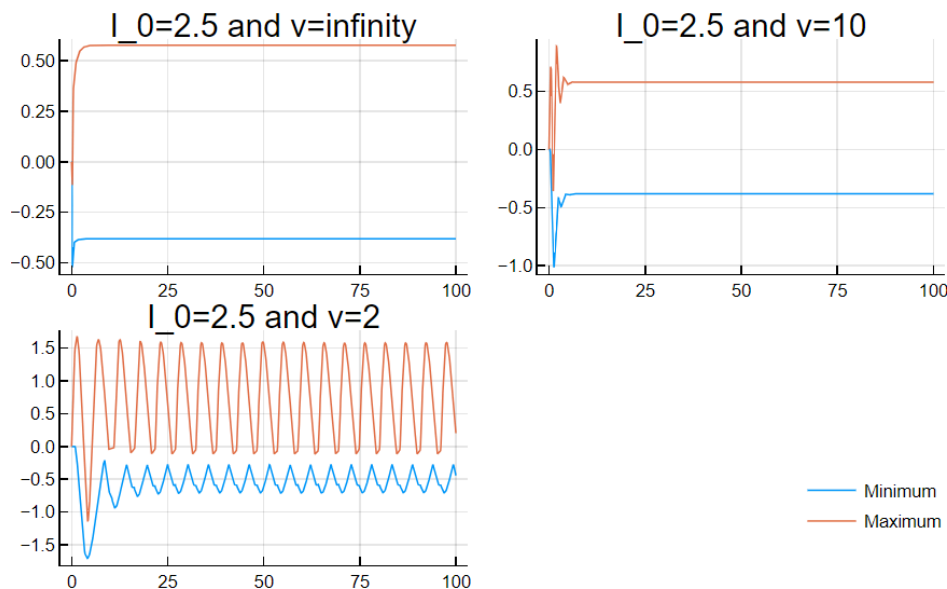


Figure 1. Plots of $\max_V(t)$ and $\min_V(t)$, in the deterministic case, for different values of the axonal speed.

In the case $I_0 = 2.5$, for example, this critical value is between $v = 2$ and $v = 3$, which indicates that there is a bifurcation point in this interval. This behaviour of the solution is illustrated by fig. 1.

If we change the external input amplitude I_0 , the location of this bifurcation also changes. In table (1) we show how the value of T_0 changes with v and I_0 . In the cases where no figures are given this means that the solution oscillates during the whole time interval. It is interesting to observe that the bifurcation occurs at low axonal speeds for high ($I_0 \geq 2$) or low amplitudes ($I_0 \leq 0.05$) of the external input; for moderate amplitudes, it occurs at higher speeds.

Table 1. Dependence of T_0 on the finite axonal velocity v and external input strength I_0 .

Velocity	T_0								
	$I_0 = 0.05$	$I_0 = 0.3$	$I_0 = 0.5$	$I_0 = 0.8$	$I_0 = 1$	$I_0 = 1.5$	$I_0 = 2$	$I_0 = 2.5$	$I_0 = 3$
∞	2.9	1.7	1.6	1.6	1.7	2.7	2.2	0.8	0.4
10	5.7	6.4	7.1	8.2	8.7	6.6	5.9	5	4.3
5	12.4	28.2	—	—	—	—	—	14.7	12.4
4	17.1	—	—	—	—	—	—	24.3	18.2
3	27.1	—	—	—	—	—	—	79.3	33.2
2	—	—	—	—	—	—	—	—	51.1

Stochastic scenario

When solving the stochastic equation, we compute $n_p = 100$ independent paths in order to evaluate the mean sample solution:

$$V_{\text{mean}}(\mathbf{x}, t) = \frac{1}{n_p} \sum_{s=1}^{n_p} V_s(\mathbf{x}, t), \quad (21)$$

The noise levels considered are $\epsilon = 0.0005, 0.001$.

When considering the stochastic neural field equation, the values of T_0 change in comparison with the deterministic case, for the same values of U_0 and v , which leads to a different type of bifurcations. In order to analyse

noise-induced bifurcations, we fix $I_0 = \frac{5}{32\pi}$ and change the values of v and ϵ . The results are displayed in Table 2, showing that as the level of noise increases the bifurcation occurs at higher values of the propagation speed.

Table 2. Dependence of T_0 on the finite axonal velocity v and level of noise ϵ

Velocity	T_0		
	$\epsilon = 0$	$\epsilon = 0.0005$	$\epsilon = 0.001$
10	8	7.4	7.2
9	8.8	7.8	7.4
8	9.2	8.6	8.2
7	12.8	9.6	12
6	14.4	19.5	17.8
5	19.8	60.8	—
4	28	—	—
3	57.8	—	—
2	—	—	—

Moreover, at low transmission speed, such as $v \leq 4$, V_{mean} oscillates without reaching any stationary state within the observation period, while in the deterministic case, the delayed solutions obtained with $v = 3, 4, 5$ reach the stationary state after a certain time. Hence, the numerical experiments suggest that the bifurcation point considering $\epsilon = 0.0005$ is between $v = 5$ and $v = 4$, whereas for $\epsilon = 0.001$ is between $v = 6$ and $v = 5$.

We therefore conclude that the random disturbances play an important role in the oscillatory behaviour of the solution.

4 Conclusions

In this paper we have described a numerical algorithm to approximate a stochastic version of the delayed neural field equation and discussed some numerical results provided by this algorithm.

In first place, the numerical simulations have shown the effectiveness of the algorithm. In spite of the fine meshes used and the large number of time steps, all the computations were carried out in a personal computer with a reasonable computational cost. Even in the stochastic case, when 100 paths of the solution have to be computed, the computations took no more than a few minutes. No doubt the use of the Fast Fourier Transform was a key factor to achieve this result.

In second place, we remark that the program language Julia has proved to be a very adequate tool for the implementation of this type of algorithms. As mentioned above, the code used to carry out these numerical experiments is available through the Julia library and its description is published in [13].

Concerning the numerical simulations discussed in Sec.3, the change of the transmission velocity was used to induce a Hopf-bifurcation in the solutions.

As a first experiment we have studied the behaviour of the solution in the deterministic case, when changing v and the amplitude of the external signal I_0 . In this case, we have observed that for a large range of values of I_0 , bifurcation points occur when changing v and the velocity at which these bifurcations occur depends on I_0 .

Then we have considered the stochastic case. In this case, for a fixed value of I_0 , we have changed v and the level of noise ϵ . Again we observe that bifurcations arise at different levels of noise. As ϵ increases, the bifurcations arise at higher values of the propagation speed.

With the purpose of applying the FFT, we have used a technique (which is described in [7] and [12]) that splits the integration domain into sub-domains and then performs a convolution in each sub-domain. When the external input and the connectivity kernel have spherical symmetry (which is the case considered in the present paper), it makes sense to consider rings as such sub-domains, as done in our algorithm. In order to solve problems with different kinds of external inputs or connectivity, we will have to consider other types of sub-domains (for example, strips, if the external input depends only on one of the coordinates). Moreover, the shape of these sub-domains may have to change with time if the external input changes. Such situations were not considered so far, and will be the subject of future work. Finally we also plan to improve the convergence order of the algorithm.

This may be achieved if the Euler-Maruyama method is replaced by higher order methods for stochastic differential equations.

Acknowledgements. This work was supported by FCT, within project UIDB/04621/2020 (Center for Computational and Stochastic Mathematics <https://doi.org/10.54499/UIDB/04621/2020>).

Authorship statement. The authors hereby confirm that they are the sole liable persons responsible for the authorship of this work, and that all material that has been herein included as part of the present paper is either the property (and authorship) of the authors.

References

- [1] S. Coombes. Large-scale neural dynamics: Simple and complex. *Biol. Cybernet.*, vol. 27, pp. 731–739, 2010.
- [2] W. Erlhagen and E. Bicho. The dynamic neural field approach to cognitive robotics. *Journal of Neural Engineering*, vol. 3, pp. R36–54, 2006.
- [3] H. Wilson and J. Cowan. Excitatory and inhibitory interactions in localized populations of model neurons. *Biophysical Journal*, vol. 12, pp. 1–24, 1972.
- [4] S. Amari. Dynamics of pattern formation in lateral inhibition type neural fields. *Biol. Cybernet.*, vol. 27, pp. 77–87, 1977.
- [5] G. Faye and O. Faugeras. New results for delayed neural field equations. *Cinquième conférence plénière française de Neurosciences Computationnelles*, vol. , 2010a.
- [6] F. Attay and A. Hutt. Neural fields with distributed transmission speeds and long-range feedback delays. *SIAM Journal of Applied Dynamical Systems*, vol. 5, n. 4, pp. 670–698, 2006.
- [7] A. Hutt and N. Rougiers. Activity spread and breathers induced by finite transmission speeds in two-dimensional neural fields. *Physical review. E, Statistical, nonlinear, and soft matter physics*, vol. 82, pp. 055701, 2010.
- [8] G. Faye and O. Faugeras. Some theoretical and numerical results for delayed neural field equations. *Physica D, Nonlinear Phenomena*, vol. 239, pp. 561–578, 2010b.
- [9] A. Hutt, A. Logtina, and L. Schimansky-Geier. Additive noise-induced Turing transitions in spatial systems with application to neural fields and the Swift-Hohenberg equation. *Physica D: Nonlinear Phenomena*, vol. 237, n. 6, pp. 755–773, 2008.
- [10] A. Hutt, A. Logtina, and L. Schimansky-Geier. Stochastic center manifold analysis in scalar nonlinear systems involving distributed delays and additive noise. *Markov Processes and Related Fields*, vol. 22, n. 3, pp. 555–572, 2016.
- [11] C. Kuehn and M. G. Riedler. Large deviations for nonlocal stochastic neural fields. *Journal of Mathematical Neuroscience*, vol. 4, pp. 1, 2014.
- [12] T. Sequeira and P. Lima. Numerical simulations of one- and two-dimensional stochastic neural field equations with delay. *Journal of Computational Neuroscience*, vol. 50, pp. 299–311, 2022.
- [13] T. Sequeira. `Neuralfieldeq.jl`: A flexible solver to compute neural field equations in several scenarios. *Journal of Open Source Software*, vol. 7, pp. 3974, 2022.
- [14] T. Sequeira. *Numerical simulations of one- and two-dimensional stochastic neural field equations with delay*. PhD Thesis, Instituto Superior Técnico, University of Lisbon, 2021.
- [15] S. E. Folias and P. Bressloff. Breathers in two-dimensional neural media. *Phys. Rev. Letters*, vol. 95, pp. 208107, 2005.